8 Optimal control of state variables and set points for IM drives

8.1 Objective

At the design of drives an energetically optimal operation represents an essential point of view. Losses increase the energy requirement and produce heat which must be dissipated by additional measures and constructive efforts. Modern power electronic devices achieve efficiencies of 98%, motors of medium and high-power ratings of over 95% at the nominal working point. A different picture arises in the partial load area where the efficiency can decline considerably. Besides optimization possibilities in the hardware sector and the use of loss-optimized pulse pattern for inverter control, also the "soft" control faction is challenged to come forth with *approaches for an efficiency optimized operation*. In order to keep the analytical and realization effort within reasonable limits, only *stationary or quasi-stationary solutions* are examined.

Another question arises from the technically existing limitations of the hardware equipment with regard to currents and voltages. The control of the state variables should be designed for the drive or the motor to always being utilized as optimal as possible.

The method of the field orientation provides the tools to realize a decoupled control of rotor flux and torque by impressing torque and flux forming current components. In a speed controlled system the set point of the torque forming current is provided by the speed controller, in a torque controlled system it is an independent control quantity. Thus *the amplitude of the rotor flux or the ratio of both components, the slip frequency, remains as a degree of freedom for the optimization*.

As shown in the next sections, the exact knowledge of difficult measurable machine parameters is required for an effective optimization of the efficiency, or this optimization can only be implemented with reasonable effort by a dynamically slow control algorithm. For this reason a second optimization approach, the *torque optimal* control, becomes

interesting. The optimization goal consists here to control machine and inverter in the best possible way *from the point of view of torque production* at the given limitations, i.e. the demanded torque has to be generated by the minimal current, or the maximum torque has to be provided at limited current or limited voltage. Such an optimization strategy also will deliver a good efficiency because of the current dependency of the ohmic losses although this does not represent the optimization goal in the first place.

8.2 Efficiency optimized control

At first it is required to perform an analysis of the controllable losses. Losses in the motor appear in the form of stator and rotor copper losses, iron losses and additional losses. Additional losses are produced in the iron and copper by the non-sinusoidal field distribution, and they can be calculated with a factor of approximately 0.3 proportionally to the copper losses [Murata 1990]. A quantitative expression for the copper losses can be derived from the active power equation:

$$p_w = \mathrm{Re}\left\{\mathbf{u}_s \mathbf{i}_s^*\right\} = \frac{3}{2}\left(u_{sx} i_{sx} + u_{sy} i_{sy}\right)^{1} \tag{8.1}$$

After replacing the voltages with the help of the stator voltage equation (cf. chapter 3 and 6) this equation can be re-written in field-orientated coordinates for stationary operation in the following form:

$$p_w = \frac{3}{2}\left[R_s i_{sd}^2 + \left(R_s + (1-\sigma)R_r\right) i_{sq}^2 + (1-\sigma)\omega L_s i_{sd} i_{sq}\right] \tag{8.2}$$

The copper losses including one part for the additional losses added with the factor k_z can be separated to:

$$p_{Cu} = \frac{3}{2}(1+k_z)\left\{R_s i_{sd}^2 + \left[R_s + (1-\sigma)R_r\right] i_{sq}^2\right\} \tag{8.3}$$

According to the section 6.2.1, the iron losses can be calculated approximately to:

$$p_{Fe} = \frac{3}{2}\frac{\left(\omega_s \psi_\mu\right)^2}{R_{fe}} \tag{8.4}$$

Using $R_{fe} \approx R_{feN}\,\omega_s/\omega_{sN}$ (cf. also section 6.2.1) and $\psi_\mu \approx L_m i_{sd}$ it can be finally written for the total losses:

[1] *xy* can be either *dq* or $\alpha\beta$

$$p_v = \frac{3}{2}\left\{\left[\left(1+k_z\right)R_s + \frac{\omega_{sN}L_m^2}{R_{feN}}\omega_s\right]i_{sd}^2 + \left(1+k_z\right)\left[R_s + \left(1-\sigma\right)R_r\right]i_{sq}^2\right\} \tag{8.5}$$

Therefore the total losses can be split into an i_{sd}-dependent (flux dependent) and a torque (or i_{sq}-) dependent part, in which the partition is defined by the parameters of the machine, and the flux dependent part is a function of the stator frequency:

$$p_v = a\left(\omega_s\right)i_{sd}^2 + bi_{sq}^2 = p_{v1}(i_{sd}) + p_{v2}(i_{sq}) \tag{8.6}$$

With the side condition of a constant or given torque:

$$m_M \sim i_{sd}i_{sq} = \text{const}$$

the condition:

$$p_{v1}(i_{sd}) = p_{v2}(i_{sq}) \tag{8.7}$$

follows for the minimal total losses, i.e. the flux dependent and the torque dependent loss components must have the same value.

A clear representation of the relationship between both loss parts can be derived if it is referred to the slip frequency. The corresponding equations are obtained similarly as above:

$$p_{Cu} = \frac{3}{2}(1+k_z)(1-\sigma)L_s i_{sd} i_{sq}\left[\left(1+\frac{R_s}{(1-\sigma)R_r}\right)\omega_r + \frac{R_s R_r}{L_m^2}\frac{1}{\omega_r}\right] \tag{8.8}$$

The factored out term is proportional to the torque and can be treated as a constant for the further calculation. For the iron losses the more exact two-parameter model from the section 6.2.1 is used now which leads to the following relation:

$$p_{Fe} = \frac{3}{2}(1-\sigma)L_s i_{sd} i_{sq}\left[R_r\left(k_{hy} + k_w\omega\right)\left(2+\frac{\omega}{\omega_r}\right) + 2R_r k_w \omega_r\right] \tag{8.9}$$

The slip-dependent loss balance at two speeds with the nominal and half the nominal torque is represented corresponding to the equations (8.8) and (8.9) for an 11kW standard motor in the figure 8.1. Because of the main flux getting smaller by an increasing slip at the same torque, the iron losses behave inversely to the slip frequency. The copper losses drastically increase at small slip because of the magnetization current demand strongly increasing with higher saturation. They show a minimum and increase once more at the slip getting greater. The optimal point with respect to the total losses depends on the respective share of the iron losses. The operation at nominal speed represents the operating point with the greatest part of the iron losses in the total losses, because here the maximum stator frequency without field weakening is reached.

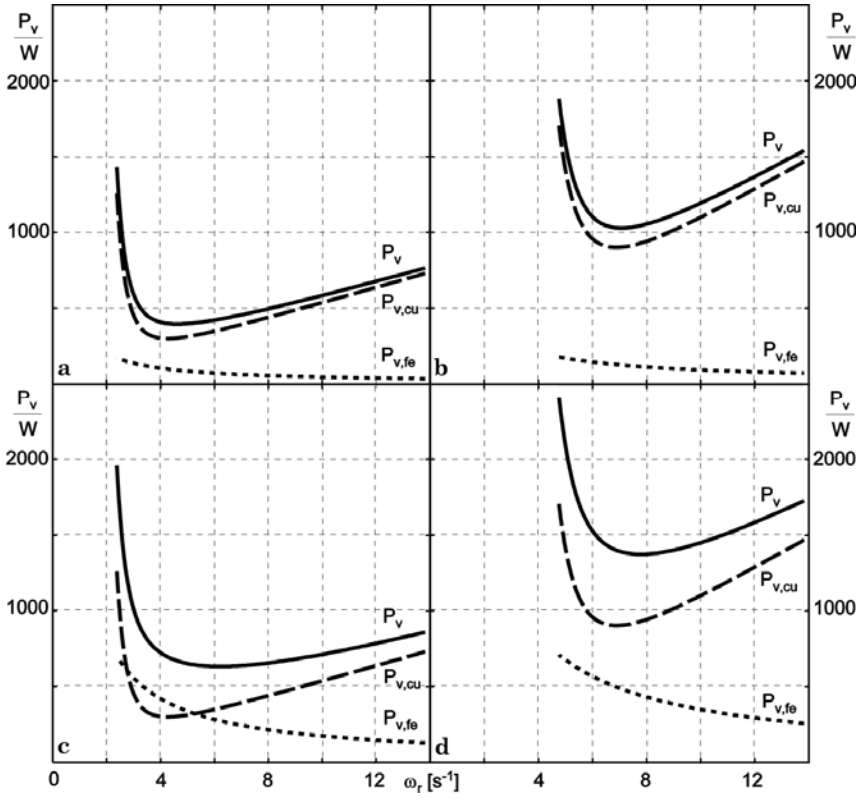

Fig. 8.1 Losses as a function of the rotor frequency: (**a**) m=0,5m_N, n=500rpm, (**b**) m=m_N, n=500rpm, (**c**) m=0,5m_N, n=1500rpm, (**d**) m=m_N, n=1500rpm

The explanations so far open up different possibilities for the practical realization of an optimal control strategy with respect to efficiency, in which the optimization goal is predefined by equation (8.7). Two variants shall be discussed in more detail.

a) Balancing of torque and flux dependent losses

The equation (8.7) shows the way for a direct control of the balance between the two parts. The method is schematically represented in the figure 8.2 (cf. [Rasmussen 1997]). The flux dependent losses can be directly controlled by the rotor flux without influencing the torque dependent losses. According to the equations (8.3) and (8.4) model values of the two loss parts are calculated. The difference of both forms the input quantity (control difference) for an I or PI controller which adjusts the equality of both parts with the rotor flux set point as a control variable.

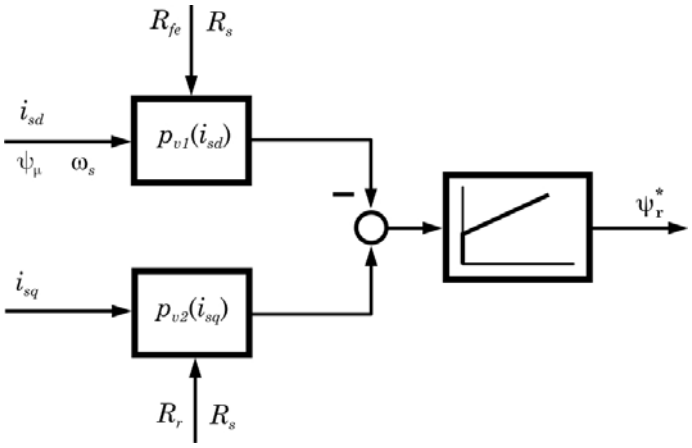

Fig. 8.2 Loss optimization by balancing of torque and flux dependent parts

A comparatively fast dynamics is achieved for adjusting the optimum, an exact compensation requires, however, an exact knowledge of the model parameters, which is difficult and requires some effort particularly with regard to the iron losses.

b) Loss compensation with search algorithm

The active power is calculated by equation (8.1), and by means of a search algorithm the rotor flux is modified until the minimum of the active power and with that the minimum of the losses is reached. Different search strategies are applicable with fixed or variable step, cf. e.g. [Moreno 1997]. A careful adjustment is required because of possible convergence problems. Such a method does not need any model parameters. Thus the power could also be measured at the input of the inverter, and the inverter losses could be included into the optimization. Caused by the searching method and the at first unknown "suitable" adjustment direction of the rotor flux, the method works slowly in this simple implementation, and is suitable exclusively for steady-state operation.

8.3 Stationary torque optimal set point generation

8.3.1 Basic speed range

Initially it shall be noted, that the relations discussed in this section are not exclusively limited to the basic speed range. They are valid everywhere where *no limitation of the stator voltage* becomes effective,

thus also in the *field weakening area at low load*. The derivations start out, however, from the basic speed range initially because no voltage limitation occurs here in stationary operation also at the current limit.

Under this presumption maximum torque at given stator current amplitude will be achieved if the operating point is always on the maximum of the slip-torque-characteristic (cf. figure 8.3). This maximum corresponds graphically to the breakdown torque of the known torque-speed-characteristic.

The torque equation is with consideration of the main field saturation in stationary operation (cf. chapter 3):

$$m_M = \frac{3}{2} z_p \frac{L_m(i_\mu)^2}{L_m(i_\mu) + L_{r\sigma}} i_{sd} i_{sq} \tag{8.10}$$

It is easily comprehensible from (8.10) that the maximum torque will be reached at a given stator current with $i_{sd} = i_{sq}$ for constant inductances. Because of the magnetic saturation the calculation of the maximum point becomes, however, essentially more troublesome and requires the iterative solution of a nonlinear system of equations. Parts of this system are besides (8.10) the relation of the magnetization current amplitude (cf. section 6.2.3):

$$i_\mu = \sqrt{i_{sd}^2 + \left(\frac{L_{r\sigma}}{L_r} i_{sq}\right)^2} \tag{8.11}$$

the slip equation:

$$\omega_r = \frac{R_r}{L_m(i_\mu) + L_{r\sigma}} \frac{i_{sq}}{i_{sd}} \tag{8.12}$$

and the boundary condition:

$$i_s^2 = i_{sd}^2 + i_{sq}^2 \tag{8.13}$$

The figure 8.3 shows the calculated characteristics for an 11kW standard motor. The characteristic which would be obtained with constant main inductance (at the nominal working point) is drawn for comparison as dashed line.

As mentioned above, it would be the task of a torque optimal control to control the rotor flux in a way to keep the operating point always on the maximum of the torque-slip-characteristic depending on the demanded or available stator current. An online calculation of this point, however, practically has to be excluded because of the necessary iteration. Therefore it would be interesting to know, how the usual field-orientated operation with constant flux (nominal flux) fits into this analysis. The nominal value of the flux forming current would be calculated by:

$$I_{sdN} = \frac{U_N}{\sqrt{3}\omega_{sN} L_s(I_{sdN})} \tag{8.14}$$

Equation (8.14) contains an iteration which would have to be solved in the practical implementation, but in the initialization phase and not in real time.

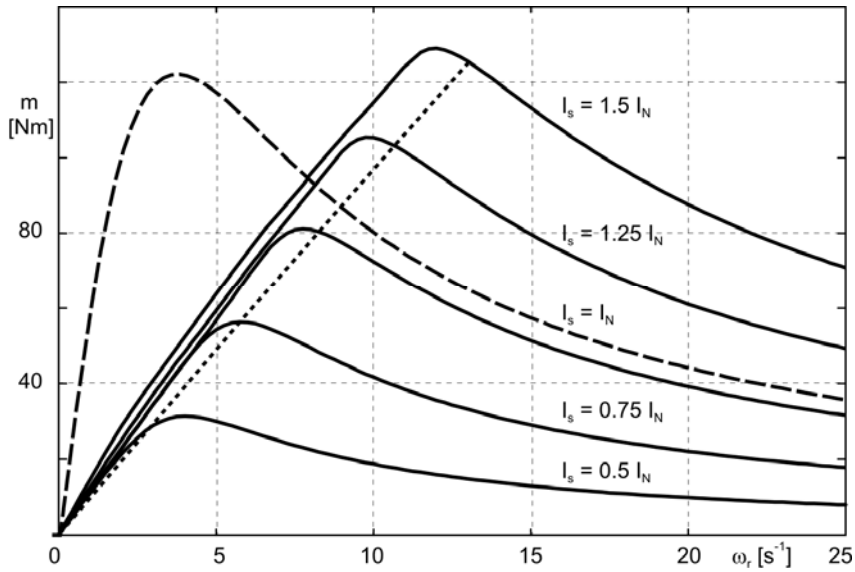

Fig. 8.3 Slip – torque – characteristic as function of the stator current amplitude: ---- L_m = const; ..... $i_{sd} = i_{sdN}$

The corresponding curve is drawn as dotted line in figure 8.3 and shows, at least at higher currents, a surprisingly good approximation to the optimal value. Therefore the constant flux operation is obviously distinguished as a quasi torque optimal control strategy in the basic speed range at higher stator currents. This connection is understandable, because the motor is designed for the rated working point.

This is further illustrated in the figure 8.4. In figure a) the necessary flux forming current to achieve the exact torque maximum and additionally the control characteristics for constant flux and for $i_{sd} = i_{sq}$ are drawn. In the linear area the optimal characteristic coincides with the characteristic $i_{sd} = i_{sq}$ as expected. For higher stator currents the optimal characteristic deviates from the constant flux characteristic with a tolerance of approximately ±20%. The figure 8.4b shows the actual effects of the deviations on the torque. Obviously they are negligible in this case.

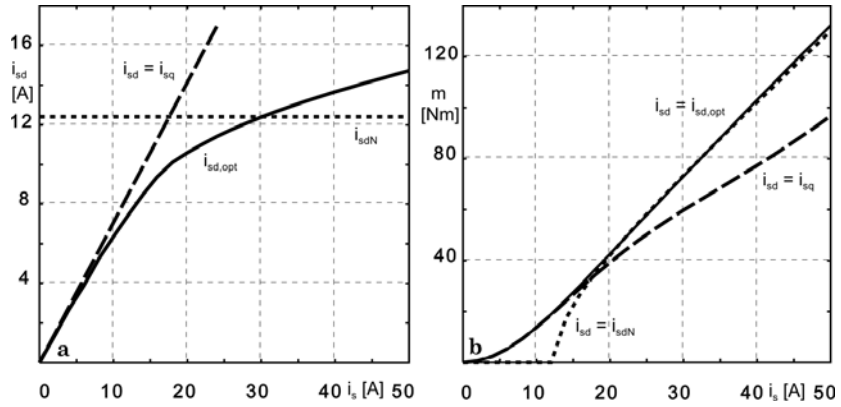

Fig. 8.4 (**a**) i_{sd} control characteristic, and (**b**) maximum torque as function of stator current and flux control

Under consideration of a minimal rotor flux which has to be kept to ensure a torque generation with an acceptable dynamics, the following simple control law can be used for the quasi torque optimal control:

$$\frac{\psi_{rd}^*}{L_m} = i_m^* = \begin{cases} i_{m,\min} & \text{for } i_{sq,f} < i_{m,\min} \\ i_{sq,f} & \text{for } i_{m,\min} \le i_{sq,f} < i_{mN} \\ i_{mN} & \text{for } i_{sq,f} \ge i_{mN} \end{cases} \tag{8.15}$$

Here $i_{sq,f}$ is the low-pass filtered current i_{sq}. Because of this filtering and the anyway existing delay in the forming of the rotor flux, a dynamic decoupling is given between flux control and i_{sq} control. It has to be taken into account, however, that a variable flux inevitably leads to a deterioration of the torque dynamics. If a high torque dynamics represents the central optimization goal, the constant flux operation has to be maintained over the complete basic speed range. The torque dynamics then only depends on the dynamics of the current impression. This is illustrated by the figure 8.5 with some transients for constant flux operation and the described flux control algorithm. In addition, it is obvious that an approximately optimal operation mode with respect to efficiency in this area is not conceivable any more with fast flux tracking in the dynamic operation.

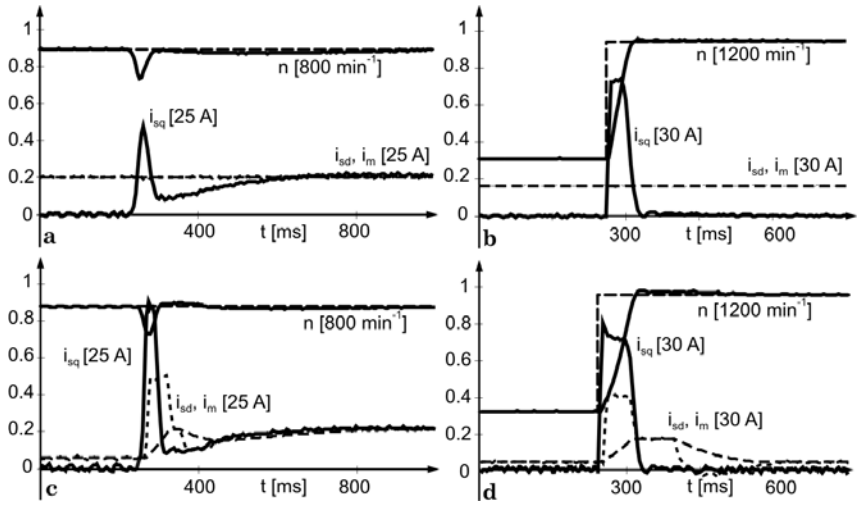

Fig. 8.5 Speed dynamics in the basic speed range: (**a**) Load step change with constant flux, (**b**) Set point step with constant flux, (**c**) Load step with torque optimal controlled flux, (**d**) Set point step with torque optimal controlled flux

8.3.2 Upper field weakening area

Different to the basic speed range, the limitation of the stator voltage represents a decisive additional influencing variable for the flux control in the field weakening. Two areas must be distinguished: The first area, in which the voltage limitation is the only deciding limiting variable, and a transition zone, in which both current and voltage limitation determine the character of the control characteristics. At first, only the voltage limitation shall be taken into account as a boundary condition, and the currents shall be assumed to develop freely.

Similar to the current-limited case, typical speed (slip) over torque characteristics can be calculated which contain the speed as a parameter. Because the calculations are only significant for the high field weakening area, the saturation can be neglected.

From the stator voltage equations in the field-orientated coordinate system (cf. chapter 3 and 6) the following equations will be obtained for steady-state operation with respect to the stator currents:

$$u_{sd} = R_s i_{sd} - \omega_s \sigma L_s i_{sq} \tag{8.16}$$

$$u_{sq} = R_s i_{sq} + \omega_s \sigma L_s i_{sd} + \omega_s (1-\sigma) L_s i_m \tag{8.17}$$

with: $i_m = \dfrac{\psi_{rd}}{L_m}$

For constant rotor flux it follows from (8.17):

$$u_{sq} = R_s i_{sq} + \omega_s L_s i_{sd} \tag{8.18}$$

The system boundary condition is here:

$$u_{\max}^2 = u_{sd}^2 + u_{sq}^2 \tag{8.19}$$

If the slip equation in field orientated coordinates (8.12) is inserted into (8.16) and (8.18) and the current components are eliminated, the following torque equation will be obtained:

$$m_M = \frac{3}{2} z_p \frac{L_m^2}{L_r} \frac{u_{\max}^2}{R_s^2} \frac{\omega_r T_r}{\left(\omega_r T_r + \omega_s T_s\right)^2 + \left(1 - \omega_s \sigma T_s \omega_r T_r\right)^2} \tag{8.20}$$

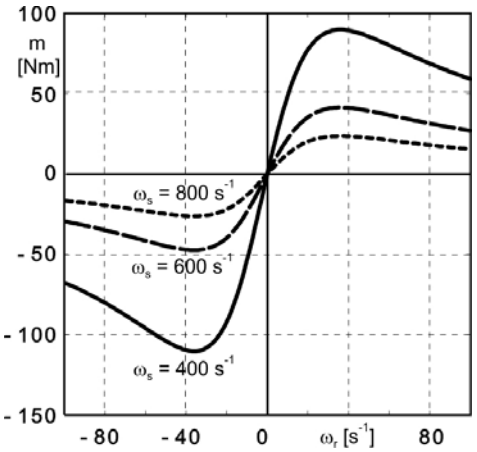

Fig. 8.6 Slip-torque characteristics at limited stator voltage; parameter: stator frequency

The equation (8.20) is represented in the figure 8.6 for the stator frequency as a parameter. This case corresponds to the natural behavior of the induction machine at frequency control. In contrast to the constant current case, differently high torque maxima, which are also characterized by differently high stator currents, appear for motor and regenerative operation. The slip frequency at the torque maximum or break-over point is calculated by (8.20):

$$\omega_{r,kipp} = \pm \frac{1}{T_r} \sqrt{\frac{1 + \left(\omega_s T_s\right)^2}{1 + \left(\sigma \omega_s T_s\right)^2}} \approx \frac{1}{\sigma T_r} \text{ for } \left(\sigma \omega_s T_s\right)^2 >> 1 \tag{8.21}$$

For speed controlled operation with the speed as a parameter the characteristics represented in figure 8.7 apply. In regenerative operation an absolute maximum at $\omega_s = 0$ appears. This means that the greatest

regenerative braking torque can obviously be generated at a (negative) direct current feeding. The torque maximum itself, however, might be barely possible to be used, because it is connected to impractical high currents.

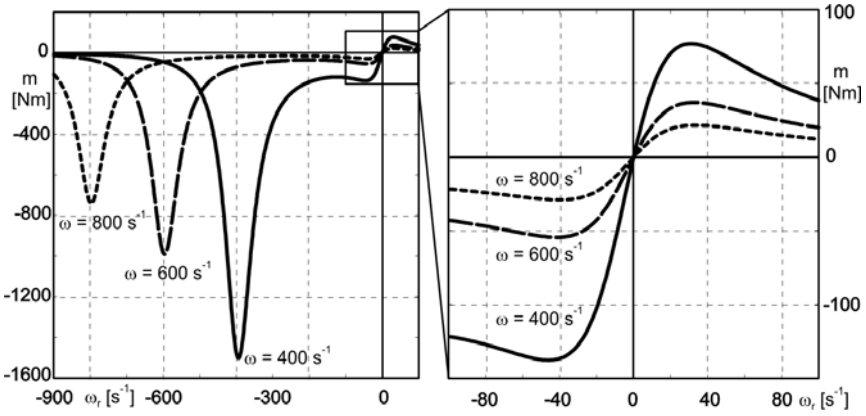

Fig. 8.7 Slip-torque characteristics at limited stator voltage; parameter: speed

Analog to the constant current operation, a torque optimal control law should adjust the currents for the maxima of the slip-torque characteristic. The solutions for the control characteristic will be obtained by an extreme value problem for the torque given by the equations (8.16), (8.18), (8.19) and the torque equation (8.10).

Because the solutions are interesting only for high stator frequencies the stator resistance can be neglected. This simplification actually makes the equation system accessible for a closed solution. Furthermore it is presupposed that because of the field weakening the main inductance can be regarded as constant.

At first, (8.16) and (8.18) have to be dissolved into components. With the mentioned simplification the following current equations are obtained (cf. equation (5.78)):

$$i_{sd} = \frac{u_{sq}}{\omega_s L_s} \tag{8.22}$$

$$i_{sq} = -\frac{u_{sd}}{\omega_s \sigma L_s} \tag{8.23}$$

Strictly speaking, the two equations also contain on the right side the current components i_{sd} and i_{sq} implicitly through the slip frequency, and would have to be solved further to equations with the speed as parameter. This would however make a closed solution impossible, whence the more

transparent variant with the stator frequency as a parameter shall be kept. The arising error is tolerable because the share of the slip frequency in the stator frequency is small at high rotational speeds. An advantage of this consists of the fact that the same control characteristics are valid for both motor and regenerative operation because of the symmetrical position of the torque maxima with respect to the slip frequency (cf. figure 8.6).

After inserting (8.22) and (8.23) into the torque equation the following Lagrange function for the extreme value calculation can be formulated by inclusion of (8.19):

$$L(u_{sd}, u_{sq}, \lambda) = m(u_{sd}, u_{sq}) + \lambda(u_{\max}^2 - u_{sd}^2 - u_{sq}^2) \tag{8.24}$$

From the partial derivatives with respect to u_{sd} and u_{sq} the following equation system is obtained:

$$0 = k_m \left(i_{sq} \frac{\partial i_{sd}}{\partial u_{sd}} + i_{sd} \frac{\partial i_{sq}}{\partial u_{sd}} \right) - 2\lambda u_{sd} \tag{8.25}$$

$$0 = k_m \left(i_{sq} \frac{\partial i_{sd}}{\partial u_{sq}} + i_{sd} \frac{\partial i_{sq}}{\partial u_{sq}} \right) - 2\lambda u_{sq} \tag{8.26}$$

with: $k_m = \frac{3}{2} z_p \frac{L_m^2}{L_r}$

After solving to the current components it yields the control characteristics:

$$i_{sd,lim} = \frac{u_{\max}}{\sqrt{2}\omega_s L_s} \tag{8.27}$$

$$i_{sq,lim} = \frac{u_{\max}}{\sqrt{2}\omega_s \sigma L_s} \tag{8.28}$$

The figure 8.8 shows these characteristics for an 11kW motor together with the characteristics calculated by means of search method without the above mentioned approximation. They are identical for both motor and regenerative operation. The maximum inverter current i_{max} and the no-load current (the magnetizing current) i_0 are also included in the plots.

In order for the torque optimal control strategy to be effective, both current components must be able to develop freely. As shown in the diagrams, this depends fundamentally on the maximum inverter current, and for the sample drive this would be the case above approximately ω_s = 450 s^{-1}. If the rotor flux is controlled below this frequency by the derived characteristic too, no torque optimal operation is achieved, because the inverter voltage cannot be utilized.

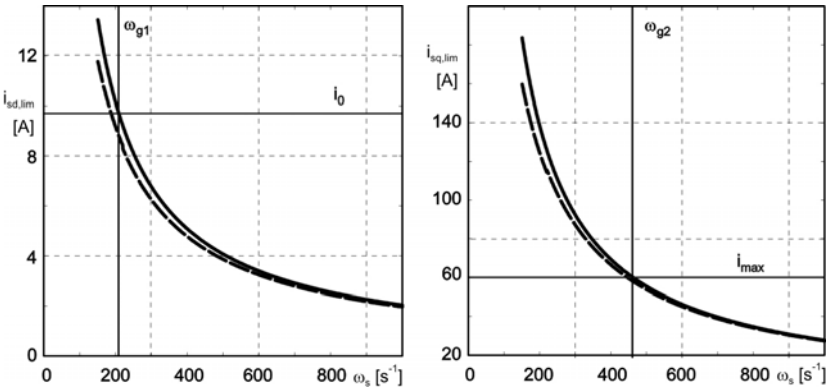

Fig. 8.8 Current limit characteristics for maximum torque at limited voltage: --- exact curve with searching method, — approximate solutions (8.27) and (8.28)

Thus it is also shown that the flux with high probability at the cut-in point of the torque optimal control characteristic may already be weakened and the operating point having been shifted to the linear part of the magnetization characteristic. Therefore the neglection of the saturation for the derivation of the characteristics is justified.

8.3.3 Lower field weakening area

The lower field weakening area shall be understood as the zone between the frequencies ω_{g1} and ω_{g2} (cf. figure 8.8). This area is indicated by the following characteristics:

- Coming from lower frequencies, the stator voltage reaches its maximum value so that a flux reduction is needed to continue the frequency increase.
- An operation using the torque optimal control characteristics is not possible or expedient, because the torque forming current i_{sq} corresponding to these characteristics is either not needed or cannot be produced.

Without voltage limitation the drive would be controlled according to the rules of the basic speed range, hence with $i_{sd} = i_{sdN}$. Thus it seems reasonable to operate the control system as close as possible at this set point in the lower field weakening area, meaning to operate the drive with the maximum possible flux at the voltage limit. This rule is well known and general practice.

For the implementation a voltage regulator is often used (figure 8.9). The actual stator voltage feedback can be calculated from the (unlimited) current controller output signal via low-pass filter to eliminate transient

parts. With that it is possible to keep the voltage always at the limiting level in stationary operation independent of motor parameters. This method has, however, also decisive disadvantages. It is attempted *to control a very fast variable quantity (stator voltage) by a slowly variable quantity* (*rotor flux)*. This demands for an artificial delay of the voltage dynamics and makes it impossible to react to variable operating states (load, acceleration) with an adequately fast change of the flux set point. For this reason a feed-forward controlled flux set point calculation shall be derived in the following.

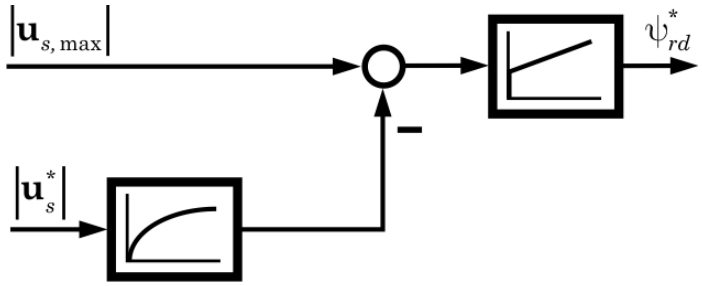

Fig. 8.9 Flux set point calculation using voltage controller

The stationary voltage equations (8.16) and (8.18) are again the starting point. The solution of the implicit relation current/stator frequency is refrained from because in this case a closed solution would require too far-reaching approximations. Both equations are squared and added up. The stator voltage amplitude is equated to the maximum voltage, and the equation is solved to $i_{sd} = i_m$. One obtains:

$$i_m^* = -\frac{(1-\sigma)R_s\omega_s L_s}{R_s^2+(\omega_s L_s)^2} i_{sq} + \sqrt{\frac{u_{\max}^2}{R_s^2+(\omega_s L_s)^2} - \left[\frac{R_s^2+\sigma(\omega_s L_s)^2}{R_s^2+(\omega_s L_s)^2} i_{sq}\right]^2} \tag{8.29}$$

For $R_s^2 << \sigma(\omega_s L_s)^2$, which should be fulfilled in the interesting frequency area ($\omega_s > 300$ s^{-1}), this relation can further be simplified. At the same time the current i_{sq} is replaced by its set point with regard to the practical implementation which enables a faster reaction to forthcoming i_{sq} changes:

$$i_m^* = -\frac{(1-\sigma)R_s}{\omega_s L_s} i_{sq}^* + \sqrt{\frac{u_{\max}^2}{(\omega_s L_s)^2} - (\sigma i_{sq}^*)^2} \tag{8.30}$$

A pure flux set point control in an open-loop has of course the disadvantage of the parameter dependency which here would have the effect, that the available stator voltage would not be utilized in stationary operation, or the flux set point would be adjusted too high. Therefore it is useful to combine both methods, voltage controller and flux feed-forward control, in a suitable way. In this combination, the voltage controller has the task of keeping the voltage at the operating limit during stationary operation, and the open-loop set point control takes care that changes of the i_{sq} set point can be answered quickly with the corresponding flux change. The voltage controller should control a quantity corresponding to its input signal. The maximum voltage $u_{\max}$ in (8.30), which is regarded as variable now, would be such a suitable quantity.

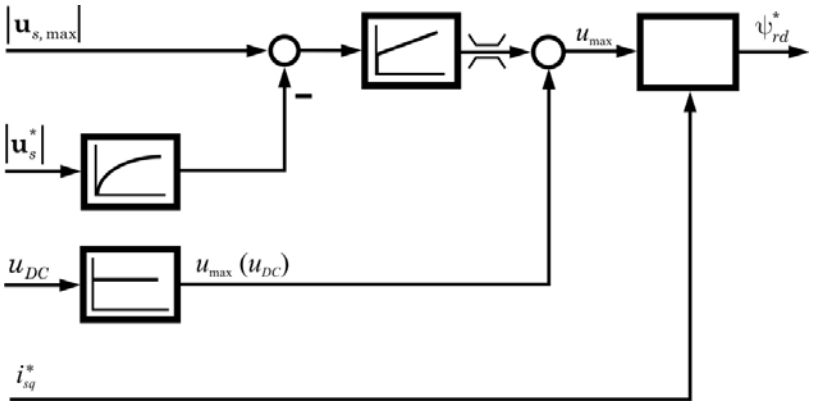

Fig. 8.10 Flux set point calculation using a combination of voltage (feedback) controller and set point control in open-loop

The figure 8.10 shows the correspondingly modified structure. The set point $u^*_{s,\max}$ corresponds to the maximum output voltage of the current controller. The control variable of the voltage controller is added to the maximum stator voltage $u_{\max}(u_{DC})$ [1)] calculated from the DC link voltage. The sum of both forms the input quantity $u_{\max}$ of the control equation.

Because the control equation (8.30) was derived in exclusively algebraic way, the saturation does not influence the result. Operating point dependent parameters can be adapted on-line by an open-loop control. Remaining differences are stationarily compensated by the voltage controller.

[1)] u_{DC} = DC link voltage

8.3.4 Common quasi-stationary control strategy

In the previous sections the theory for torque optimal control strategies has been outlined for basic speed, upper and lower field weakening area or limitation of current and/or voltage. For the implementation in a control system there are still the following additional tasks to be addressed:

- A common strategy which provides a continuous transition between the areas is to find.
- The developed strategy must be usable in a control structure, such as described in the section 1.2.

From the previous considerations the following conclusions can be summarized:

- The rules developed for the basic motor speed range can be generalized for all operating states in which no voltage limitation appears.
- The rules for the two field weakening areas show that the best utilization of the machine is always given at a maximum voltage output.
- The current limit characteristics in the upper field weakening area show such a relationship, that the limit characteristic of the torque forming current $i_{sq,lim}$ can be equated to the maximum value of the stator current with good approximation.

Therewith the following rules can verbally be formulated:

- *Rule* 1: The torque and flux forming current components are equated as long as either the flux forming current reaches its maximum value (nominal value) or the stator voltage goes into the limitation.
- *Rule* 2: If the torque forming current amplitude exceeds the flux forming current, either the flux forming current remains on its nominal value or is controlled to keep the drive always on the voltage limit.
- *Rule* 3: The stator current is limited to either its absolute maximum or the limit characteristic of the torque forming current in the upper field weakening area, depending on which of both quantities has the smaller value.

With the nominal value of the rotor flux linkage i_{mN} and the maximum inverter current i_{max} the rules can be summarized in equation form as follows:

$$i_m^* = \begin{cases} i_{m,\min} & \text{for } i_{sq,f} < i_{m,\min} \\ i_{sq,f} & \text{for } i_{m,\min} \le i_{sq,f} < i_{mN} \text{ and } i_{sq,f} < i_m^*(u_{\max}, i_{sq}^*, \omega_s) \\ i_{mN} & \text{for } i_{sq,f} \ge i_{mN} \text{ and } i_{mN} < i_m^*(u_{\max}, i_{sq}^*, \omega_s) \\ i_m^*(u_{\max}, i_{sq}^*, \omega_s) & \text{otherwise} \end{cases} \tag{8.31}$$

$$i_{s,\max} = \begin{cases} i_{\max} & \text{for } i_{sq,\lim} > i_{\max} \\ i_{sq,\lim} & \text{otherwise} \end{cases} \tag{8.32}$$

The quantity $i_m^*(u_{\max}, i_{sq}^*, \omega_s)$ results from the equation (8.30). The rules or the control laws start out from the assumption that the set point i_{sq}^* exists as an independent input quantity. They will appear somewhat more complicated and contain components to be calculated possibly in iteration if the torque is immediately provided as a set point. In the configuration with superimposed speed control looked at here, the adjustment of the torque is subjected to the speed-feedback control loop.

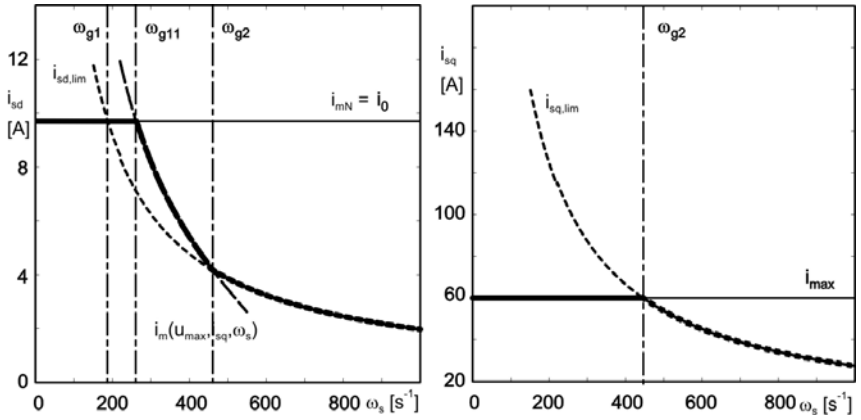

Fig. 8.11 Current limit characteristics for the torque optimal operation and maximum voltage output

The current limit characteristics are represented in expansion of figure 8.8 in figure 8.11 corresponding to the proposed algorithm for the complete speed range. The differences are recognizable clearly in the transition zone: The cut-in point of the field weakening is shifted to the frequency ω_{g11}, the maximum flux range is extended to substantially higher stator frequencies then defined by the torque optimal characteristic.

With this control, the area of the utilizable torque-speed range represented in the figure 8.12 for the first quadrant finally results. This area is delimited by the available current in the basic speed range, at high rotational speeds by the ceiling speed of the motor, and as discussed in the upper field weakening area by the available voltage, in the lower field weakening area by the maximum current and maximum voltage. The transition point between the upper and lower field weakening areas in turn is given by the frequency ω_{g2}.

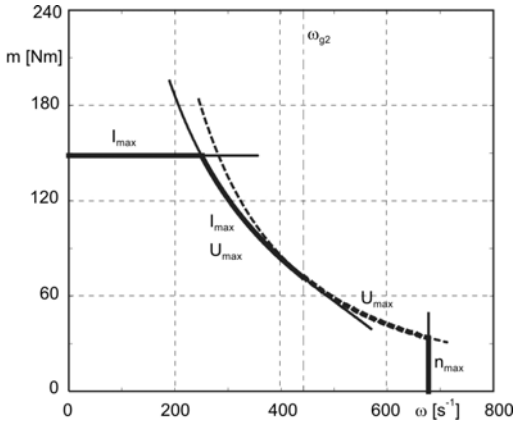

Fig. 8.12 Utilizable torque-speed range

The difference in the operating behaviour between torque optimal operation and conventional flux control can be shown best with the results of a practically realized control. For this purpose a speed reversal process is most suitable because quasi-stationary conditions (slowly variable currents and flux linkages) can be found here in wide areas. The comparison is made using a control characteristic of the form:

$$i_m^* = 0.9 i_0 \frac{\omega_N}{\omega} \frac{\sqrt{3} U_{s,\max}}{U_N} \frac{L_{mN}}{L_m} \tag{8.33}$$

$$i_{s,\max} = i_{\max} \tag{8.34}$$

i.e. a flux characteristics, which is inversely proportional to the speed, and which adapts to changes of the DC link voltage and the main inductance. The plots of the most interesting quantities are shown in the figure 8.13. The differences in the reversal time are significant. An essential difference consists in the fact that *although the stator voltage with torque optimal control under load permanently resides at its limit during field weakening, the current controller predominantly, works in the linear area*. On the other hand *the controllability of the system is temporarily lost with the simple flux control*. It shall not remain unmentioned that similar results like those of the torque optimal control can be achieved also with a simple flux control in favorable parameter constellation and choice of the field weakening cut-in with respect to the reversal time. The temporary loss of the system controllability under loads is, however, hardly avoidable.

Furthermore it has to be noticed that a dynamically correct flux model (with saturation, cf. sections 6.2.3 and 4.4.1) is strongly necessary for the successful realization of the flux control algorithms.

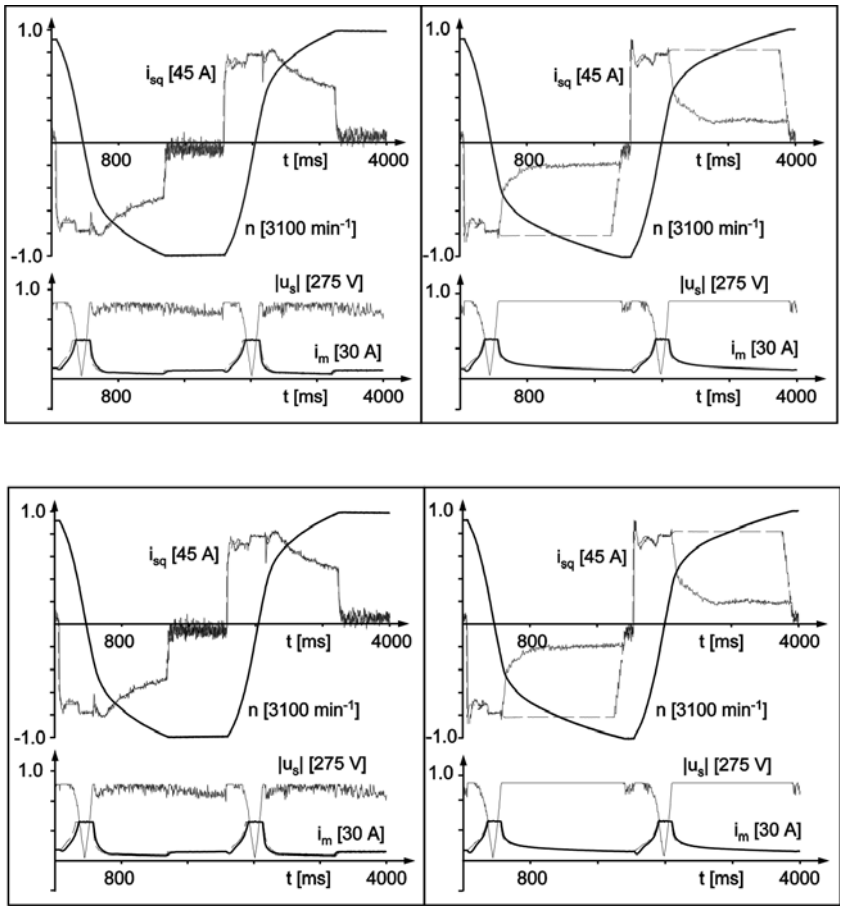

Fig. 8.13 Speed reversal processes +3100 rpm ↔ -3100 rpm: torque optimal control (**left**) and speed inverse flux control (**right**)

8.3.5 Torque dynamics at voltage limitation

As long as a sufficient voltage reserve is available, the torque dynamics is primarily a question of fast current impression. In the field weakening area this problem appears to be fundamentally more complex because of the missing voltage reserve. Regarding this the optimization goal consists here in reaching a rise time as short as possible also at the boundary condition of the limited voltage.

One of the outstanding features of the FOC consists in the possible high-dynamic impression of the torque because the torque rise time, constant rotor flux assumed, is identical with the rise time of the torque forming

current. Prerequisite for a fast current impression is an adequate voltage reserve, though, so that a really fast torque impression is only possible in the basic speed range. According to the above derived rules, no voltage reserve would be available in the field weakening area at all. It is therefore necessary before an intended stepping-up of the torque to produce this voltage reserve by a (dynamic) flux reduction. The whole process should take place at unchanged maximum stator voltage for an optimal utilization of the machine.

After squaring and adding-up of (8.16) and (8.17) and neglection of R_s at the same time, the following equation is obtained:

$$u_s^2 = \left(\omega_s \sigma L_s i_{sq}\right)^2 + \left(\omega_s \sigma L_s i_{sd} + (1-\sigma)\omega_s L_s i_m\right)^2 \tag{8.35}$$

From this relation it is recognizable that a dynamic control reserve can, considering the slow variability of i_m, be created by reducing the component i_{sd}. The derivation of the control law must, however, start out from the dynamically correct voltage equations. In the first instant the rotor flux linkage is constant changes compared to the stator current only very slowly, and therefore has influence on the calculation as a parameter and not as a variable. Regarding the searched-for current set point i_{sd}^* quasi-stationary conditions can be assumed, and therefore the leakage time constant can be neglected. Furthermore it is assumed that the current transients are progressing approximately linearly and therefore the stator resistance is also negligible. The leakage inductance in the q axis must not be neglected however, because after the current i_{sd}^* to be calculated is reached, the decisive i_{sq} transient will unfold. Thus the initial equations are:

$$u_{sd} = -\omega_s \sigma L_s i_{sq} \tag{8.36}$$

$$u_{sq} = \frac{\sigma L_s}{T_q}\Delta i_{sq} + \omega_s \sigma L_s i_{sd} + (1-\sigma) L_s \omega_s i_m \tag{8.37}$$

The parameter T_q is the time needed by the i_{sq} transient, and represents a free design parameter in certain limits (see below). Δi_{sq} is the difference between the actual and the set point value. Both equations are squared, added-up and solved to i_{sd}:

$$i_{sd}^* = \frac{1}{\sigma}\left[-(1-\sigma) i_m - \frac{\sigma \Delta i_{sq}}{\omega_s T_q} + \sqrt{\left(\frac{u_{\max}}{\omega_s L_s}\right)^2 - \left(\sigma i_{sq}\right)^2}\right] \tag{8.38}$$

The radix expression in (8.38) shall be abbreviated to i_{m1}. The equation (8.38) is then:

$$i_{sd}^{*} = \frac{1}{\sigma}(i_{m1} - i_m) + i_m - \frac{\Delta i_{sq}}{\omega_s T_q} \tag{8.39}$$

In the stationary state the last term disappears, and i_{sd}^{*} is equal to i_m. Therewith i_{m1} has also to be equal to i_m and can be understood as the stationary flux set point. The stationary set point for maximum voltage is provided normally by (8.30). Therefore also this value could be used instead of i_{m1} in (8.39) resulting in a sliding transition between dynamic and stationary flux control.

With respect to its structure, the equation (8.39) is comparable with an integral controller. The reciprocal leakage coefficient forms the controller gain, and the last term can be interpreted as an additional disturbance compensation. Nothing speaks against using this "controller" instead of the usual flux controller. *Caution is just necessary for machines with very small leakage factor and great sampling period of the flux control* because the controller gain then can accept inadmissible high values. In this case a PI flux controller may be used in stationary operation.

The determination of T_q must be carried out empirically. The influence of this parameter becomes clear by the simulation examples shown in the figure 8.14. A set point step of the torque forming current and thus of the torque was applied from zero to maximum for an acceleration process at about the double nominal speed. The sampling period T of the current control is 0.5 ms. The sampling period of the flux set point generator, flux and speed control is 2 ms. The optimum for T_q is found to approximately $T_q = 20T$ and valid for the complete field weakening area. Further reduction brings no benefit for the reduction of the rise time, just increases the overshooting of i_{sq}.

At the beginning of the transient a temporary drop of the torque forming current (and therewith the torque) appears. This is understandable because at first the voltage required for the impression of i_{sd} can only be gained at the expense of the voltage in q direction.

The rise times of the torque are in the area of 5....6 ms. It must not remain unmentioned that to obtain the shown transients besides the optimal set point generation a current controller is required which can impress the current components with the necessary dynamics and precision. The state-space dead-beat controller described in section 5.4 fulfills these prerequisites.

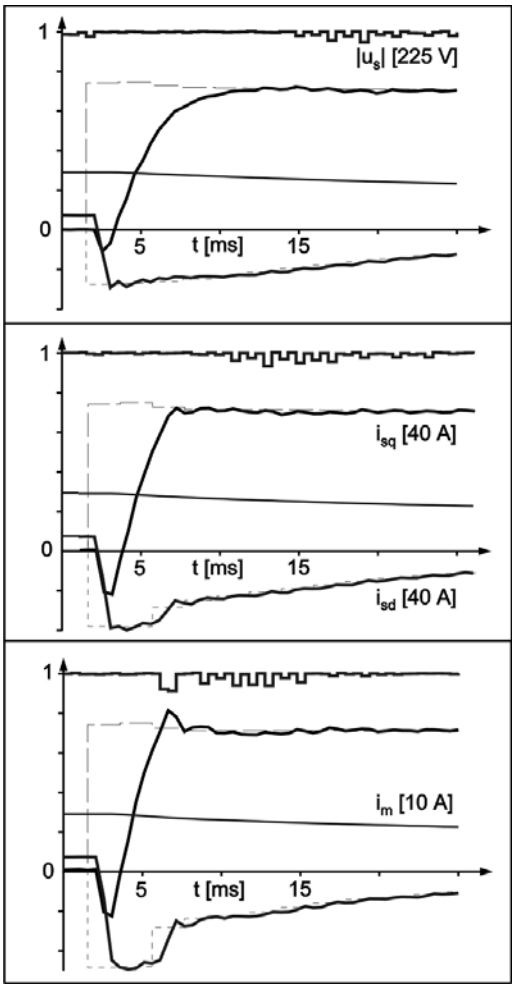

Fig. 8.14 Torque impression at maximum voltage: $T_q = \infty$ (**top**), $20T$ (**middle**), $10T$ (**bottom**), $\omega = 700\text{s}^{-1}$

Satisfactory results at the practical implementation fundamentally depend on the precision of the model parameters. A dynamically correct rotor flux model is required as an essential component. The figure 8.15 shows results from a sample drive. Because of the voltage maximum practically only one current component is actually controlled (in motor operation i_{sd}), all model inaccuracies and simplifications or unbalance and offset errors are mirrored in the second current component. The rise time of the torque forming current component confirms the values obtained by simulation.

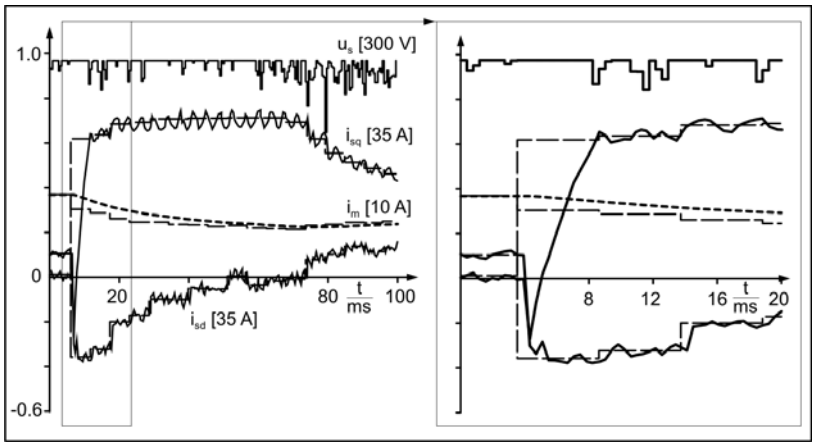

Fig. 8.15 Torque impression at voltage maximum, $\omega_s = 500\ s^{-1}$

It has to be remarked that the described method manages with relatively moderate computation power. As shown by the figure 8.15, the current control works with a sampling time of 0.4 ms; the flux set point calculation, the flux and speed control are realized with a sampling time of 5 ms.

8.4 Comparison of the optimization strategies

Starting point of this chapter was the control of the state of the IM under the objective of energy optimal operation. The torque optimal control was introduced because of the advantages in the dynamic case and under the aspect of current and voltage limitation. In connection with this, it is interesting to compare the control methods with regard to the efficiency actually achieved.

The achieved efficiency for the different control methods is represented for the sample drive (11kW motor) in the figure 8.16. The curves for efficiency optimal and torque optimal control are approximately identical at loads above the half rated torque, because the total losses are dominated by the copper losses. The control with constant rotor flux also reaches the efficiency of the other methods at high torque, because the slip gets close to the optimal value (cf. section 8.3.1). Significant differences arise at medium and low torques, though. Here obviously the decisive possibilities for improvements by using optimized methods are to be found. For the examined example, the efficiency optimal control achieves visible differences compared to torque optimal control only at high speeds and

small loads, because the share of the iron losses is here the biggest one. Also the values of the approximated torque optimal control described in the section 8.3.2 are only sparsely below those of the exact method. At higher loads a decrease of the efficiency can be found for all methods because of the increasing total current. This trend is more distinctive at smaller speeds, because the loss minimum shifts to lower slip values due to lower iron losses, and the main field saturation is reached earlier.

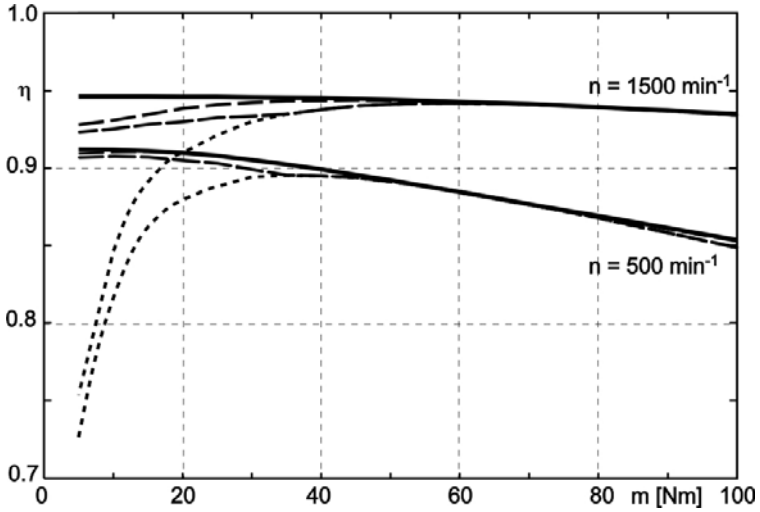

Fig. 8.16 Load-dependent efficiency for different control methods: ——— efficiency optimal control; - - - - - torque optimal control, exact calculation; ····· constant rotor flux (= nominal flux); - - - - - (thin line) torque optimal control, approximated calculation

This behaviour can also be comprehended from the figure 8.17 in which the control characteristics for rotor flux and magnetizing current depending on the torque and speed are represented for the efficiency optimal and torque optimal control. Also here it can be recognized, that distinctive differences in the control characteristics only appear at high speeds and according share of the iron losses. The characteristics for torque optimal control are as expected independent of the speed, and insignificantly different from the efficiency optimal control at small speeds.

In the example, a rotor flux slightly higher than the nominal flux adjusts itself at high torques. The increase of motor voltage caused by this accompanying effect of the optimal control necessitates a voltage-dependent limitation of the rotor flux. Thus the optimum operation would be no longer practicable near the nominal operating point.

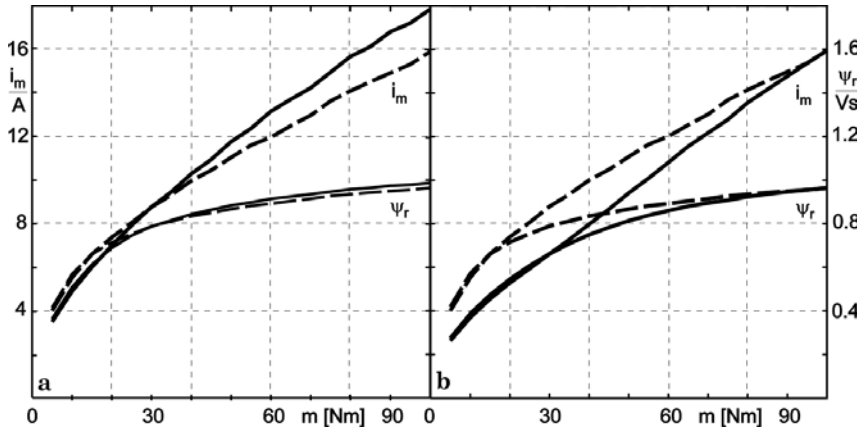

Fig. 8.17 i_m and ψ_r at torque optimal and efficiency optimal control: ——— efficiency optimal control; ····· torque optimal control; (**a**) n = 500 min^{-1} (**b**) n = 1500 min^{-1}

In the field weakening area, the efficiency optimal operation will once more approach the torque optimal operation because of the strongly reduced iron losses. Thus noticeable efficiency improvements by an efficiency optimal control remain limited to the upper area of the basic speed range at low load. This statement is valid of course under the assumption that the ratio between copper and iron losses approximately corresponds to the one of the motor used for the calculations.

The following can be summarized to compare the control methods with respect to the efficiency behaviour:

- As opposed to constant flux operation the torque optimal control (optimization on minimal stator current at given torque) already delivers a considerable improvement particularly in the partial loads area.
- Further possibilities for efficiency improvement using a loss-optimal control strategy confine to the upper basic speed range at partial loads, and account to some per cent for usual ratios of iron and copper losses. The absolute loss reduction is even lower because visible effects are only obtained in the low load area.
- Further system boundary conditions like voltage and current limitation, which largely determine the optimization capabilities, come into play in the field weakening area. The iron losses decrease strongly with flux reduction.
- An exact optimization requires in any case iterative on-line calculations, because of the magnetic saturation, and measuring of the iron loss characteristic for loss-optimal operation. At least for the torque optimal

operation, however, simple control laws can be derived, which avoid these two problems and match the results of the exact control very closely.

Altogether, the torque optimal operation represents a very effective and recommendable control method also with respect to efficiency optimization. The efficiency optimal operation is generally recommendable if all optimization reserves have to be utilized (high motor power). It offers itself for stationary operation as an addition in form of an active power controller outlined in the section 8.2.

8.5 Rotor flux feedback control

The last section of this chapter deals with the rotor flux control in concentrated form because the calculated flux set points would be realized by a flux control loop according to the control structures discussed in chapter 1. Appropriately, the control is designed in the field-orientated coordinate system.

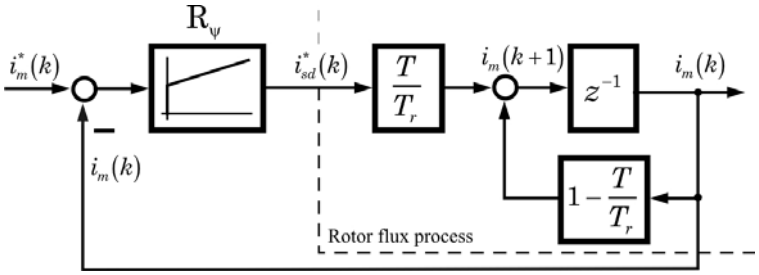

Fig. 8.18 Flux control loop with inner current loop

As described in the chapter 5, the inner-loop current control is optimized for finite adjustment times, and runs compared to the flux control with a considerably shorter sampling period of characteristically T_i/T_ψ>0.1. Therefore the current impression can be regarded undelayed with respect to the flux control, and the actual controlled process is given by the rotor voltage equation in field-orientated coordinates (cf. chapter 3 and 6):

$$0 = i_m + T_r \frac{\mathrm{d}\, i_m}{\mathrm{d}\, t} - i_{sd} \tag{8.40}$$

It can be written in time-dicrete form:

$$i_m(k+1) = \left(1 - \frac{T}{T_r}\right) i_m(k) + \frac{T}{T_r} i_{sd}(k) \tag{8.41}$$

The current component i_{sd} forms the control variable. The control loop is represented in the figure 8.18. The flux controller is generally designed as a PI controller (digital magnitude optimum) and quasi-continuously optimized for transfer behaviour. If a PI controller is assumed with the equation:

$$\mathrm{R}_{\psi}(z) = V_{\psi}\frac{1-d_{\psi}\,z^{-1}}{1-z^{-1}} \tag{8.42}$$

then the magnitude-optimal setting for the flux controller is:

$$V_{\psi} \approx \frac{1}{3\left(1-e^{-T_{\psi}/T_r}\right)};\; d_{\psi} \approx e^{-T_{\psi}/T_r} \tag{8.43}$$

T_{ψ} = Sampling period of the flux controller; T_r = Rotor time constant

The figure 8.19 shows a transient process with magnetization and the following motor start-up up to the field weakening area, and illustrates the transient response of the flux at magnitude optimum.

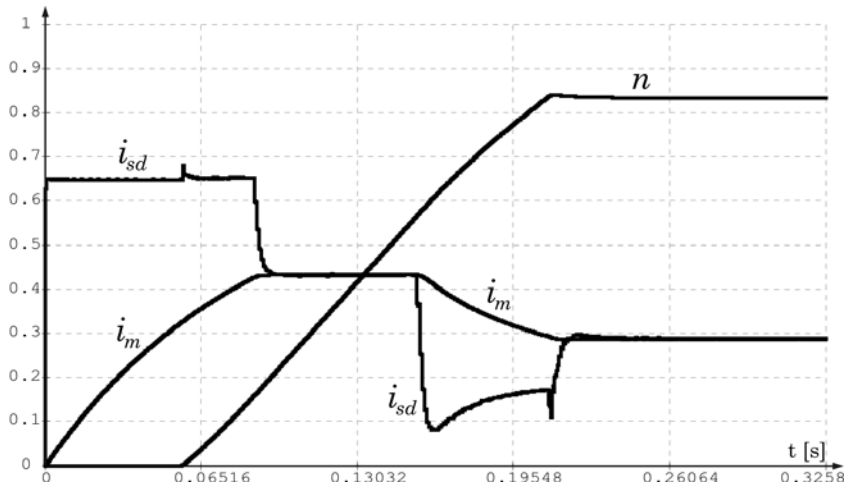

Fig. 8.19 Transient response of the flux at magnitude-optimal setting for the flux controller

A second approach for the flux controller, especially in connection with the optimization strategy discussed in this chapter, immediately arises from the control equation (8.39) for i_{sd} derived in the section 8.3.5 for the dynamically torque optimal current impression at the voltage limit. The equation is rewritten as follows:

$$i_{sd}^{*}(k) = i_m(k) + \frac{1}{\sigma}\left[i_m^{*}(k) - i_m(k)\right] \tag{8.44}$$

The compensation term, dependent on the i_{sq} control error, was neglected because this term is only required for a fastest possible torque dynamics at the voltage limit. If the first term on the right side would not read $i_m(k)$ but $i_{sd}^{*}(k\text{-}1)$ (what is fulfilled in the stationary operation), the equation (8.44) would describe an I controller with the controller gain $V_I = 1/\sigma$.

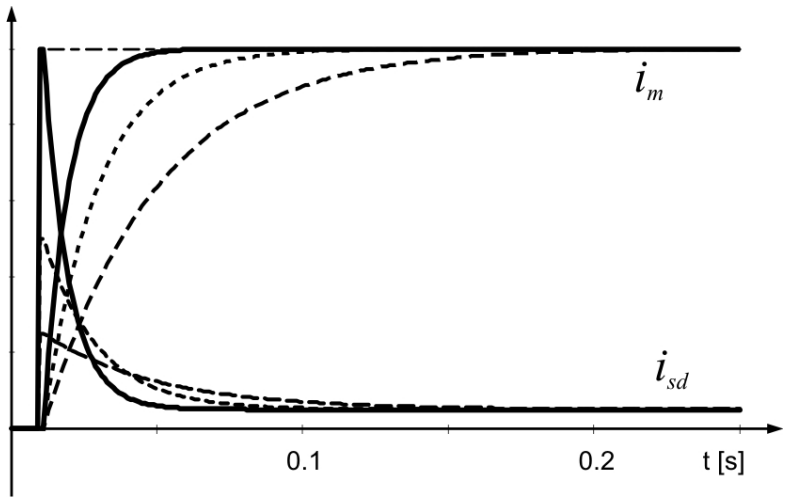

Fig. 8.20 Transient response of closed flux control loop with quasi-I controller

As shown in the figure 8.20, the closed control loop has in small signal operation approximately the transfer behaviour of a first-order delay function, in which the rise time is predefined by the controller gain. The unusual feature of the design consists in the fact that because of $V_I = 1/\sigma$ the dynamics does not have to be predefined by "external" optimization rules, but is determined by the "point of view of the torque impression". For a very small leakage factor the controller gain can become too big, though, and cause unstable behaviour together with the amplitude quantization, hence a limit of V_I = 15...20 should be set. On the other hand, if the dynamics of the controller is to be adapted to certain needs, nothing would speak against a deviation from the implicit setting $V_I = 1/\sigma$.

8.6 References to chapter 8

Dittrich JA (1998) Anwendung fortgeschrittener Steuer- und Regelverfahren bei Asynchronantrieben. Habilitationsschrift, TU Dresden

Moreno-Eguílaz JM, Cipolla M, Peracaula J (1997) Induction Motor Drives Energy Optimization in Steady and Transient States: A New Approach. EPE Trondheim, pp. 3.705 - 3.710

Khater-Faeka MH, Lorenz RD, Novotny DW, Tang K (1991) Selection of Flux Level in Field-Oriented Induction Machine Controllers with Consideration of Magnetic Saturation Effects. IEEE Transactions on Industry Applications, Vol. IA-27, No. 4, July/August, pp. 720 – 726

Maischak D, Németh Csóka M (1994) Schnelle Drehmomentregelung im gesamten Drehzahlbereich eines hochausgenutzten Drehfeldantriebs. Archiv für Elektrotechnik 77, S. 289 – 301

Murata T, Tsuchiya T, Takeda I (1990) Quick Response and High Efficiency Control of the Induction Motor Based on Optimal Control Theory. 11. IFAC World Congress, Tallin, vol. 8, pp. 242 – 247

Rasmussen KS, Thogersen P (1997) Model Based Energy Optimizer for Vector Controlled Induction Motor Drives. EPE Trondheim, pp. 3.711 - 3.716

Vogt G (1985) Digitale Regelung von Asynchronmotoren für numerisch gesteuerte Fertigungseinrichtungen. Springer-Verlag

Wiesing J (1994) Betrieb der feldorientiert geregelten Asynchronmaschine im Bereich oberhalb der Nenndrehzahl. Dissertation, Uni. Paderborn